
Article:
Abu, A.K., Burgess, I.W. and Plank, R.J. (2013) Tensile Membrane Action of Thin Slabs Exposed to Thermal Gradients. Journal of Engineering Mechanics, 139 (11). pp. 1497-1507. ISSN: 0733-9399

https://doi.org/10.1061/(ASCE)EM.1943-7889.0000597

The Effect of Reinforcement Ratios on Composite Slabs in Fire

Anthony K. Abu[*]*, Ian W. Burgess[†], Roger J. Plank[‡]

Abstract

Public-domain software is currently available in order to allow designers to incorporate the enhancement of fire resistance due to tensile membrane action of composite slabs into their analysis of building behaviour in fire. It embodies an updated simplified calculation model based on the Bailey-BRE Method for the design of composite slab panels for the fire limit state. It optimises reinforcement size to generate an enhanced slab capacity at large deflections, so that it is capable of bearing the fire limit state loading at the required fire resistance time, expressed in terms of an allowable-deflection limit. The method assumes that protected edge beams maintain absolute vertical support of the slab panel at its boundaries, only allowing for failure of compartmentation integrity by tensile fracture of mid-panel reinforcement or by concrete crushing at the corners. However, these protected edge beams deflect under their enhanced loading in fire, which can cause a structural failure of the slab panel before the required fire resistance time. It is therefore imperative to determine the real contribution of the area of reinforcement to tensile membrane action, given adequate consideration of the loss of vertical edge support. This paper, as an extension to a previous paper on the effects of protected edge beams on slab tensile membrane action, presents a series of finite element studies conducted with the software *Vulcan*, compared with the current Bailey-BRE Method and the public-domain TSLAB software, to determine the influence of reinforcement area on the failure of slab panels at elevated temperatures.

Keywords: buildings, structures & design; composite structures; design methods & aids; fire engineering; slabs & plates; steel structures; thermal effects

[*] Department of Civil and Natural Resources Engineering, University of Canterbury, Private Bag 4800, Christchurch 8140, New Zealand
[†] Department of Civil and Structural Engineering, University of Sheffield, Sir Frederick Mappin Building, Mappin Street, Sheffield S1 3JD, United Kingdom
[‡] School of Architectural Studies, University of Sheffield, The Arts Tower, Western Bank, Sheffield S10 2TN, United Kingdom
* Corresponding author: Email: tony.abu@canterbury.ac.nz

1 Introduction

Recent trends aimed at ensuring the fire resistance of structures have encouraged increased use of performance-based approaches, which are now often categorised as structural fire engineering. These methods attempt to model, to different degrees, the actual behaviour of the three-dimensional structure, taking account of realistic fire exposure scenarios, the loss of some load from the ultimate to the fire limit state, actual material behaviour at elevated temperatures and interaction between various parts of the structure. Assessment of the real behaviour of structures in fire has shown that the traditional practice of protecting all exposed steelwork can be wasteful in steel-framed buildings with composite floors, since partially-protected composite floors can generate sufficient strength to carry considerable loading at the fire limit state, through a mechanism known as tensile membrane action, provided that fire-compartmentation is maintained and that connections are designed with sufficient strength and ductility. Tensile membrane action is a load-bearing mechanism of thin slabs under large vertical displacement, in which an induced radial membrane tension field in the central area of the slab is balanced by a peripheral ring of compression. In this mechanism the slab capacity increases with increasing deflection. This load-bearing action offers economic advantages for composite floor construction, since a large number of the steel floor beams can be left unprotected. The conditions necessary for the effective use of this mechanism are two-way bending and vertical support along the slab's edges. In the current UK structural fire engineering implementation of performance-based methods, buildings are designed to comply with a list of agreed acceptance criteria, including a range of typical fires, causing realistic temperatures of the beams, columns and slabs, allowable deflection limits to avoid integrity failure, and acceptable connection forces at elevated temperatures. These requirements make nonlinear finite element methods ideal for structural fire engineering assessments, as the behaviour of an entire building (or a substantial part of it) can be monitored. However, numerical analyses are time-consuming processes, and so simplified methods which provide good preliminary estimates of structural behaviour are always an advantage.

The BRE membrane action method, devised by Bailey and Moore (2000), is one such procedure, which assesses composite slab capacity in fire by estimating the enhancement which tensile membrane action makes to the flexural capacity of the slab.

It is based on rigid-plastic theory with large change of geometry. The method assumes that a composite floor is divided into rectangular fire-resisting "slab panels" (see Fig. 1), composed internally of parallel unprotected composite beams, vertically supported at their edges which usually lie on the building's column grid. In fire the unprotected steel beams within these panels lose strength, and their loads are progressively borne by the highly deflected thin concrete slab in biaxial bending. The increase in slab resistance is calculated as an enhancement of the traditional small-deflection yield-line capacity of the slab panel. This enhancement is dependent on the slab's aspect ratio, and increases with deflection. The method, initially developed for isotropically reinforced slabs (Bailey, 2000), has been extended to include orthotropic reinforcement (Bailey, 2003). A more recent update by Bailey and Toh (2007a) considers more realistic in-plane stress distributions and compressive failure of concrete slabs. The deflection of the slab has to be limited in order to avoid an integrity (breach of compartmentation) failure. Failure is defined either as tensile fracture of the reinforcement in the middle of the slab panel or as compressive crushing of concrete at its corners. The deflection limit, shown as Equation (1), is defined on the basis of thermal and mechanical deflections and test observations:

$$v = \frac{\alpha(T_2 - T_1)l^2}{19.2h} + \sqrt{\frac{0.5 f_y}{E}_{t=20°C} \times \frac{3}{8} L^2} \qquad (1)$$

in which:

- v is the allowable vertical displacement
- α is the coefficient of thermal expansion of concrete
- T_2 is the slab bottom surface temperature
- T_1 is the slab top surface temperature
- L is the length of the longer span of the slab
- l is the length of the shorter span of the slab
- h is the effective depth of the slab, as given in BS EN1994-1-2 Annex D (BSI British Standards, 2005)
- f_y is reinforcement yield stress
- E is the elastic modulus of the reinforcement

The first term of Equation (1) accounts for the "thermal bowing" deflection, assuming a linear temperature gradient through the depth of a horizontally-unrestrained concrete slab. The second part considers deflections caused by applying an average tensile mechanical reinforcement strain, of 50% of its yield strain at 20°C, across the longer span of the slab, assuming that its horizontal span stays unchanged. This part of the allowable deflection is further limited to $l/30$. In normal structural mechanics terms this superposition of two components of the total deflection is not acceptable, because of their incompatible support assumptions, but nevertheless it is the deflection limit used. The limiting deflection has been calibrated to accord with large-scale fire test observations at Cardington (Bailey, 2000). In particular, in Equation (1) α is taken as 18×10^{-6}/°C, the recommended constant value (BSI British Standards, 2005) for simple calculation, for normal-weight concrete, and the difference (T_2-T_1) between the bottom and top slab surface temperatures is taken as 770°C for fire resistance periods up to 90 minutes, and 900°C for 2 hours, based on the test observations (Bailey, 2001).

A primary advantage of the method is the simplicity of its calculations; it is therefore suitable for implementation in spreadsheet software. The Steel Construction Institute (SCI) has further developed the method, and has implemented it in the Microsoft-Excel-based spreadsheet TSLAB (Newman *et al.*, 2006). Whereas the basic method limits slab deflections using the assumption of nominal temperatures based on the Cardington fire tests, the vertical deflection limit in TSLAB is calculated by using T_2 and T_1 values obtained from a thermal analysis of the slab cross-section. A plot of the limiting deflections from the two processes, for a 9m x 9m x 130mm deep normal-weight concrete slab panel cast on ComFlor 60 steel decking, is shown in Fig. 2. The deflection limits are compared against the general *(span/20)* deflection criterion which is the upper limit in the Standard Fire test (BSI British Standards, 1987). It is observed that, although TSLAB embodies the calculation process of the Bailey-BRE Method, there are differences between their limits. A direct comparison of the two approaches has also indicated (Toh and Bailey, 2007) that there are discrepancies between the original Bailey-BRE equations and their interpretation in TSLAB. On inspection it is evident that, not only does the Bailey-BRE limit assume a constant temperature difference between the top and bottom surfaces of the slab, but it also uses a higher coefficient of thermal expansion for normal-weight concrete than that used in TSLAB.

The Bailey-BRE Method and TSLAB both assume that full vertical support is available at all the slab panel boundaries. In practice, this is achieved by protecting the slab panel's edge beams, which must lie on the column grid of the building (see Fig. 1). When the unprotected secondary beams lose most of their strength at very high temperatures there is a re-distribution of the loads carried by these protected edge beams; the primary beams lose load because of the loss of load capacity of the unprotected beams whose ends they support, whereas the protected secondary beams gain load by tending to support the floor area with which they would be associated in a non-composite two-way-spanning slab. The Bailey-BRE method therefore requires that the protected secondary beams are designed for their increased load ratios at the fire limit state. As the protected beams lose strength with time, and the load re-distribution at the Fire Limit State causes increased deflections at the panel boundaries, the assumption of continuous vertical support along the panel's edges becomes progressively less valid. The use of yield-line theory as the baseline for the strength enhancement also dictates that a slab panel's capacity increases with increased reinforcement area unless duly arrested by a compressive failure criterion, as identified by Bailey and Toh (2007). However, since the primary requirements for tensile membrane action to be mobilised are double-curvature bending, large deflections and vertical edge support, excessive deflections of the protected edge beams can result in the double-curvature bending being converted into single-curvature bending. In consequence the panel may fail structurally in sagging, so that the reinforcement's tensile strength is not usefully employed.

Previous studies by Bailey and Toh (2007), Huang *et al.* (2002, 2004b) and Foster (2006) have compared the Bailey-BRE method both with experiments and with more detailed analytical approaches based on finite element analysis. These have highlighted a number of shortcomings in the simplified method. One which has attracted particular interest is the effect of increased slab reinforcement ratios. The Bailey-BRE method indicates that a modest increase in the reinforcement ratio can result in a disproportionately large increase in composite slab capacity, whereas the finite element analyses indicate a much more limited increase. The finite element studies by Huang *et al.* (2002, 2004b) examined slabs with some continuity along their edges. The Bailey-BRE method was developed assuming that slab reinforcement

fractures in hogging over its edge supports, leaving simply-supported edges which allow horizontal pull-in. Recent research (Abu *et al.*, 2008, Abu, 2009) has shown that the behaviour of edge beams affects the failure mode and failure time of slab panels in fire. For panels which lie on the perimeter of a building, the lack of in-plane and rotational restraint along their free edges implies a reliance on the selection of reinforcement area and adequate sizing and protection of edge beams.

This paper extends the investigation of the effects of edge beam behaviour on slab panel failure (Abu *et al.*, 2008) by examining the effects of increasing reinforcement areas. The study is conducted by comparing results from *Vulcan* finite element analyses of isolated slab panels with those of the Bailey-BRE method, in order to determine the influence of reinforcement area on slab panels at elevated temperatures, and to identify the range of applicability of the method's assumptions. The paper does not include material type, ductility, surface texture or orthotropic reinforcement effects on slab panel failure. It is clear that these could significantly influence the behaviour of these panels, as observed by Foster *et al.* (2004) and Bailey and Toh (2007b). With practical structural fire engineering design in mind, the comparisons are done with respect to the deflection criteria of TSLAB, the original Bailey-BRE Method and the Standard Fire Test (l/20).

2 Studies comparing *Vulcan* and the Bailey-BRE Method

The three slab panel layouts shown in Fig. 3 were used for the structural analyses. The 9m x 6m, 9m x 9m and 9m x 12m panels were designed for 60 minutes' standard fire resistance, assuming normal-weight concrete of cube strength 40MPa and a characteristic imposed load of 5.0kN/m^2, plus 1.7kN/m^2 for ceilings and services. Using the trapezoidal slab profile shown in Fig. 4, the requirements of SCI P-288 (Newman *et al.*, 2006) and the slab specifications given in Table 1, the floor beams were designed according to BS 5950-3 (BSI British Standards, 1990) and BS 5950-8 (BSI British Standards, 2003), assuming full composite action between steel and concrete, and simple support to all beams, in line with common British engineering practice. The "Office" usage class is assumed, so that the partial safety factors applied to loadings are 1.4 (dead) and 1.6 (imposed) for ULS and 1.0 and 0.5 for FLS. The

assumed uniform cross-section temperatures of the protected beams were limited to 550°C at 60 minutes. The ambient- and elevated-temperature designs resulted in specification of the steel beam sizes shown in Table 2.

As previously mentioned, the assessment in this paper is presented as a comparison between the Bailey-BRE method and *Vulcan* finite element analysis. Both the Bailey-BRE Method and TSLAB implicitly assume that the edges of a slab panel do not deflect vertically. The progressive loss of strength of the intermediate unprotected beams is captured by a reduction in the steel yield stress with temperature. The reduced capacity of the unprotected beams (interpreted as an equivalent floor load intensity) is compared with the total applied load at the Fire Limit State to determine the vertical displacement required by the reinforced concrete slab (whose yield-line capacity also reduces with temperature) to generate sufficient enhancement to carry the applied load. The required displacement is then limited to an allowable value. The *Vulcan* finite element analysis, on the other hand, properly models the behaviour of protected edge beams, with full vertical support available only at the corners of each panel. *Vulcan* Huang *et al.*, 2003a, 2003b, 2004a) is a three-dimensional geometrically nonlinear specialised finite element program which also considers nonlinear elevated-temperature material behaviour. Nonlinear layered rectangular shell elements, capable of modelling both membrane and bending effects, are used to represent reinforced concrete slab behaviour, while beam or column behaviour is adequately modelled with segmented nonlinear beam-column elements. The different layers and segments of the elements can be assigned different temperatures, with corresponding thermal strains and stress-strain characteristics in fire, thereby giving the elements the capability to model the effects of differential thermal expansion in a structure. Concrete failure follows a biaxial peak-stress interaction surface assuming "smeared" cracking.

The analyses are initially performed with the standard isotropic reinforcing mesh sizes A142, A193, A252 and A393. These are respectively composed of 6mm-, 7mm-, 8mm- and 10mm-diameter bars of 500N/mm^2 yield strength, all at 200mm spacing. The required mid-slab vertical displacements of the Bailey-BRE approach and the corresponding predicted deflections of the *Vulcan* analyses are compared with the TSLAB, BRE and Standard Fire Test (l/20) deflection limits; the structural properties of the two models are selected to be consistent with the assumptions of the Bailey-BRE

Method (Bailey, 2001). The results are also compared with a simple slab panel failure mechanism (Abu, 2009), shown in Fig. 5. This mechanism determines the time at which the horizontally unrestrained slab panel loses its load-bearing capacity due to biaxial tensile membrane action, and goes into single-curvature bending (simple plastic folding), due to the loss of plastic bending capacity of the protected edge beams. Using a work-balance equation, it predicts when the parallel arrangements of primary or secondary (intermediate unprotected and protected secondary) composite beams lose their ability to carry the applied fire limit state load because of their temperature-induced strength reductions. The expressions for plastic folding failure across the primary and secondary beams are shown in Equations (2) and (3) respectively:

Primary beam failure

$$\frac{wab}{2} - \frac{4\sum M_p}{a} \geq 0 \qquad (2)$$

Secondary beam failure

$$\frac{wab}{2} - \left(\frac{4\sum M_s}{b} + \frac{4\sum M_u}{b} \right) \geq 0 \qquad (3)$$

In the equations above a and b are the lengths of the primary and secondary beams; w is the applied fire limit state floor loading and M_u, M_s and M_p are the temperature-dependent capacities of the unprotected, protected secondary and protected primary composite beams, respectively, at any given time.

The observations from early analyses led to a more detailed investigation of the combined effects of edge-beam stability and the reinforcement ratios on slab panel failure in fire. For the most like-against-like comparison against Bailey-BRE and TSLAB, the slab panel temperature conditions generated by TSLAB needed to be reproduced in the *Vulcan* analyses. The unprotected intermediate beam temperatures from TSLAB were also applied directly to the other two models. TSLAB generates weighted mean temperatures of the slab top surface, bottom surface and reinforcement. These were applied directly to the Bailey-BRE models. The same could not be assumed for the *Vulcan* analyses, as fictitious temperatures would have needed to be assumed for

the other layers in the slab's cross-section. These assumptions could adversely influence both thermal and stress-related strains in the model. Thus, following the earlier research (Abu *et al.*, 2008), a one-dimensional thermal analysis of the average depth (100mm) of the profiled slab was performed with the software FPRCBC-T (Huang *et al.*, 1996). The temperatures (shown in Fig. 6) correlated very closely with those from TSLAB. These temperatures were applied in the *Vulcan* analyses.

3 Results

The results of the comparative analyses, shown in Figs. 7-9, show slab panel deflections with different reinforcement mesh sizes. For ease of comparison, in each graph the A142-reinforced panels are shown as dotted lines, while those reinforced with A193, A252 and A393 are shown as dashed, solid and chain-dot lines respectively. For clarity the required vertical displacements for the Bailey-BRE Method and the predicted actual displacements from the *Vulcan* analyses are shown on separate graphs ('a' and 'b') for each slab panel size. Displacements predicted by *Vulcan* at the centres of the slab panels are also shown relative to the deflections of the midpoints of the protected secondary beams in graphs 'c' for comparison. This illustration is appropriate because the deflected slab profile in the Bailey-BRE method relates to non-deflecting edge beams; a more representative comparison with *Vulcan* therefore requires a relationship between its slab deflection and deflected edge beams. Further, this approach has the advantage of de-congesting the figures for more accurate interpretation. The limiting deflections, and the times at which plastic folding of the slab, including the protected edge beams, takes place (referred to as the 'collapse time') are also shown. Regardless of the layout of a panel, it can be observed that the single-curvature fold line always occurs across secondary beams; the associated collapse times are indicated by the vertical lines in the figures. The temperatures of the various intermediate and protected secondary beams at failure for the three slab panel layouts are shown in Table 3. Apart from the 9m x 6m panel it can be seen that failure occurs when the protected secondary beams are below their own limiting temperatures (see Table 2). The results are discussed in terms of slab aspect ratio (defined as *Longer slab span /shorter slab span*), and the panel capacity with respect to each limiting deflection. It is to be expected that

square slab panels should have the highest enhancement of their capacity due to tensile membrane action.

3.1 Slab panel analyses

9m x 6m Slab Panel

SCI P-288 (Newman *et al.*, 2006) specifies A193 as the minimum reinforcing mesh required for 60 minutes' fire resistance. Fig. 7(a) shows the required Bailey-BRE displacements together with the deflection limits and the slab panel collapse time. A193 mesh satisfies the BRE limit, but is inadequate for 60 minutes' fire resistance according to TSLAB. A252 and A393 satisfy all deflection criteria. It should be noted that there is no indication of failure of the panels according to Bailey-BRE, even when the collapse time is approached. This is partly due to their neglect of the behaviour of the edge beams; runaway failure of Bailey-BRE panels is only evident in the required deflections when the reinforcement has lost a very significant proportion of its strength. *Vulcan* predicted deflections are shown in Fig. 7(b). It is observed that the A393 mesh just satisfies the BRE limiting deflection at 60 minutes. It can also be seen that the deflections of the various *Vulcan* analyses converge at the 'collapse time' (82min) of the simple slab panel folding mechanism. This clearly indicates the loss of bending capacity of the protected secondary beams. Comparing Figs. 7(a) and 7(b), the Bailey-BRE Method predicts substantial enhancement of the panel fire resistance with increasing reinforcement mesh size, while *Vulcan* shows a marginal increase. Also the Bailey-BRE approach is found to be conservative with A142 and A193 and unconservative with the larger mesh sizes. As the slab panel edges in the Bailey-BRE and TSLAB methods are assumed to stay vertical, the required displacements shown in Fig. 7(a) should be considered as relative values. Relative displacements of the slab centre with respect to the deflected protected secondary beams in the *Vulcan* model are shown in Fig. 7(c). If this principle is accepted, a comparison of Figs. 7(a) and 7(c) indicates that the Bailey-BRE predictions for A142 and A193 are conservative. Results for A252 in these two figures correlate closely. However, for A393, the Bailey-BRE method appears unconservative. Further examination of Fig. 7(c) shows that A252 and A393 meshes satisfy all the limiting deflection criteria, while A193 is adequate according to the TSLAB and BRE limit criteria. It should be noted that a reduction in

the relative displacement is an indication of incipient runaway failure of the slab panel, since the deflection of the protected secondary beams begins to catch up with that of the unprotected intermediate beams, forming a single-curvature failure mechanism by folding of the whole panel.

9m x 12m Slab Panel

In the previously-discussed 9m x 6m slab panel the secondary beams are longer than the primary beams. In the 9m x 12m layout this is reversed. However, its large overall size requires its minimum mesh size to be A252 (Newman *et al.*, 2006). From the required displacements shown in Fig. 8(a), A252 mesh satisfies a 60-minute fire resistance requirement with respect to the Bailey-BRE limit. It is observed from this graph that increasing the mesh size from A252 to A393 results in an increase in the slab panel capacity from about 37min to over 90min, relative to the TSLAB deflection limit. The same cannot be said for the *Vulcan* results (Fig. 8(b)), which show very little increase in capacity with larger meshes. It is shown that A252 and A393 meet the fire resistance requirement at 60 minutes with respect to the BRE limiting deflection. It is also observed that the *Vulcan* deflections appear to converge on a slab panel collapse time of 68min. At failure, the protected secondary beams are at 594°C, which is considerably below their limiting temperature. Note that, in this study, sufficient protection is applied to all protected beams to ensure that their design temperature (at 60 minutes) is limited to 550°C. Typically in an economic design, beams would be protected to a temperature just below their critical temperature at the required fire resistance time. This would potentially cause structural failure of the panel earlier than 68min. The displacement of the centre of the panel relative to the mid-span deflection of the protected secondary beams is shown in Fig. 8(c). A393 mesh is seen to satisfy all deflection criteria, while A193 and A252 satisfy the TSLAB and BRE limits. Comparing Figs. 8(a) and 8(c), the Bailey-BRE method is the more conservative of the simplified procedures. However it is important to note that the use of relative deflections may require either heavy protection of edge beams or limitation of their deflections to Standard Fire test deflection limits (*l/20*).

9m x 9m slab panel

Fig. 9 shows results for the 9m x 9m slab panel, plotted together with the edge beam collapse mechanism and the three deflection criteria. The discrepancy between the Bailey-BRE limit and TSLAB is evident once again; the recommended minimum reinforcement for 60 minutes' fire resistance, A193, is adequate with respect to the BRE limit, but fails to meet the TSLAB limit. As reported for the other panel layouts, an increase in mesh size results in a disproportionately large increase in the Bailey-BRE panel resistance (Fig. 9(a)) while *Vulcan* (Fig. 9(b)) shows a more modest increase. Failure of the protected secondary beams at 73min (also Fig. 9(b)) limits any contribution the reinforcement might have made to the panel capacity. A comparison of the relative displacements (Fig. 9(c)) with the required Bailey-BRE displacements indicates that the latter method is the more conservative for A142 and A193 meshes.

The comparisons in Figs. 7-9 show that finite element modelling indicates only marginal increases in slab panel capacity with increasing reinforcement size. The Bailey-BRE method, on the other hand, shows huge gains in slab panel resistance with larger mesh sizes, even when compared to the relative displacements given by the finite element analyses. Results for the 9m x 6m and 9m x 9m slab panels have shown that the Bailey-BRE method is conservative with the lower reinforcement sizes, while it overestimates slab panel capacities for higher mesh sizes. The 9m x 12m panel, however, requires higher reinforcement sizes in any case. The *Vulcan* results show that slab panel capacity is affected more by geometry than by reinforcement area. Better correlations were recorded between the required displacements and relative displacements from the finite element model than with absolute displacements. However, the use of relative displacements in assessing slab panel capacity should be considered in conjunction with an evaluation of the capacity of protected edge beams. There is a need to incorporate the effect of edge beams into the simplified Bailey-BRE analysis, and so a more detailed study of the effect of reinforcement area relative to slab panel failure is now undertaken.

3.2 Effects of reinforcement ratio

The comparison in the previous section shows that the Bailey-BRE Method can predict very high increases of slab panel capacity as a result of small changes in reinforcement area, while *Vulcan* on the other hand indicates only marginal increases. The fact that the structural response of the protected secondary beams is ignored seems to be the key to this over-optimistic prediction by the Bailey-BRE Method. Therefore, to investigate the real contribution of reinforcement ratios, structural failure of the panel as a whole by plastic folding has been incorporated as a further limit to the Bailey-BRE deflection range. Fictitious intermediate reinforcement sizes have been used, in addition to the standard meshes, in order to investigate the effects of increasing reinforcement area on slab panel resistance. The range of reinforcement area is maintained between 142mm^2/m and 393mm^2/m; the additional areas are 166, 221, 284, 318 and 354 mm^2/m. The investigation in this section examines failure times of the slab panel with respect to the three limiting deflection criteria (TSLAB, the generic BRE limit and *Span/20*) normalised with respect to the time to creation of a panel folding mechanism, since this indicates a real structural collapse of the entire slab panel. Results for the 9m x 6m, 9m x 12m and 9m x 9m panels are shown in Fig. 10. The lightly-shaded curves show required deflections from the Bailey-BRE Method. The deflections predicted by *Vulcan* are shown as darker curves. The dotted, solid and dashed lines refer respectively to failure times with respect to the *short span/20* criterion, the TSLAB deflection limit and the BRE limit.

Fig. 10(a) shows how the normalised 9m x 6m slab panel failure times vary with increasing reinforcement mesh size for the 60-minute design case. The results confirm the earlier observation of modest increases in slab panel capacity in the finite element model and over-optimistic predictions in the Bailey-BRE Method model. Looking at the BRE limit, the increase in slab panel resistance between reinforcement areas of 142mm^2/m and 166mm^2/m is 26%. However, increasing the reinforcement area from 166mm^2/m to 193mm^2/m results in a capacity increases of over 100%. Similar observations are made with respect to the other deflection limits with reinforcement areas above 200mm^2/m. *Vulcan* on the other hand registers a maximum capacity increase of only 30% between 142mm^2/m and 393mm^2/m. A comparison of the two

analytical models shows that the Bailey-BRE Method is conservative in this case up to a reinforcement area of about 200mm^2/m for the 9m x 6m slab panel. A similar trend is observed for the 9m x 12m slab panel (Fig. 10(b)). However, this large panel requires a larger area of reinforcement to mobilise tensile membrane action. Thus the conservatism of the Bailey-BRE Method extends to about 300mm^2/m, depending on the selection of the deflection limit. The *Vulcan* failure times also increase rapidly between 142mm^2/m and 250mm^2/m and experience a gradual increase thereafter, indicating that a minimum reinforcement area is necessary to realise the effects of tensile membrane action. A comparison of normalised failure times for the 9m x 9m slab panel with respect to reinforcement area is shown in Fig. 10(c). The effect of the square aspect ratio is evident. The *Vulcan* analysis records an increase in slab panel capacity of 97% between 142mm^2/m and 393mm^2/m relative to the TSLAB limit. The Bailey-BRE Method on the other hand indicates that a 60-minute slab rating can be achieved with isotropic reinforcement mesh area between 166mm^2/m and 250mm^2/m.

The comparisons in Fig. 10 further confirm that the Bailey-BRE Method is conservative for the lower areas of reinforcement, but is otherwise unconservative. The method depends on the calculation of an enhancement to the small-deflection yield-line capacity which increases with increasing reinforcement size. Disproportionately higher slab capacities are obtained with higher reinforcement ratios, if the capacity of the protected edge beams is not adequately considered. The results show that the finite element analyses give a more logical indication of the contribution of the reinforcement area to slab panel capacity. The *Vulcan* 60-minute analyses show a steady increase in slab resistance with increasing reinforcement area, as they realistically consider the behaviour of edge beams and the failure properties of concrete and reinforcement. For a more general assessment of the effect of reinforcement on slab panel failure, 90- and 120-minute fire resistance design scenarios are now examined with *Vulcan*.

The 9m x 6m, 9m x 12m and 9m x 9m slab panels are re-designed for these higher fire resistance times by selecting appropriate beam sizes, fire protection and slab thicknesses to ensure that the load ratios of all beams lie between 0.4 and 0.5, considering increased loadings on the protected secondary beams at the fire limit state. Also, the reinforcement depth is maintained at 45mm from the top surface of the slab. Again the fire protection ensures that the protected beam temperatures reach a

maximum of 550°C at the respective fire resistance times, on exposure to the standard fire curve. The beam specifications for the 90- and 120-minute cases are shown in Table 4. The slab panel collapse times and corresponding intermediate and protected secondary beam temperatures are shown in Table 5. *Vulcan* Failure times for the 9m x 6m, 9m x 12m and 9m x 9m slab panels with respect to the TSLAB, BRE and *Span/20* deflection limits for 60-, 90- and 120-minute panels are plotted together in Fig. 11. Since the 60-minute designs have already been highlighted in Fig. 10, they are shown as thinner lines, in the background of each figure. The line codings used in the previous figure are maintained for Fig. 11.

From Fig. 11(a), it is seen that lower reinforcement area does not significantly influence slab panel failure times for the 90- and 120-minute cases. Mesh sizes above 280mm^2/m show significant increases in capacity with increasing reinforcement. A similar trend is observed in the 9m x 12m slab panel (Fig. 11(b)). An examination of the results of the 9m x 9m slab panel in Fig. 11(c) reveals a general increase in failure time with increasing reinforcement area. However, it is observed that mesh sizes below 240mm^2/m hardly influence slab panel capacity, especially in the higher fire resistance category. To investigate the phenomenon further four extra fictitious reinforcement mesh sizes (236.5, 244.25, 260 and 268 mm^2/m) are included in the 120-minute 9m x 9m slab panel analyses. By examining the failure time curve relative to the TSLAB deflection limit for the 120-minute design scenario, even with the increased number of reinforcement areas, it is evident that two conditions exist for failure. The same phenomenon is however not recorded in the 60-minute case (Fig. 10(c)), which shows a continuous increase in slab panel capacity with increasing reinforcement size.

For tensile membrane action to be the most significant load-carrying mechanism, the unprotected beams need to lose considerable strength. This commences when a temperature of 400°C is attained. However, for unprotected beam load ratio of 0.467, corresponding to a limiting temperature of 622°C, the slab panel system behaves as a set of individual composite beams until the stage where the individual unprotected beams lose significant load-bearing resistance and deflect rapidly, ultimately reaching the point where the slab, in biaxial bending, relies on tensile membrane action to bear the applied loading. After reaching the limiting temperature of the composite secondary beams, large deflections develop in the central area of the slab, allowing transfer of load

to membrane action of the slab. Typically, the unprotected beams in the 120-minute 9m x 9m slab panel are at 740°C at about 25min and deflect rapidly. Lower reinforcement areas are unable to arrest this deflection before the TSLAB deflection limit is reached (Fig. 12). However this is not observed with the higher reinforcement areas such as A393, as they contribute more to the initial bending resistance of the slab, thereby allowing it to utilise fully the extra capacity that membrane action provides, hence increasing the failure time. Although the increased thickness in the 120-minute panel reduces the thermal gradient in the slab, its restrained in-plane expansion, against much colder perimeter beams, induces higher initial deflections than in the 60-minute model. In addition, the '*h*' term in Equation (1) increases, thereby reducing the vertical deflection limits of TSLAB and BRE, thus causing early 'failure' of the less highly reinforced panels and implying higher minimum reinforcement areas for higher fire resistance times.

In tensile membrane action the extent of the central tensile area is an indication of the tensile capacity of the slab. For a given reinforcement size, an increase in the central tensile area is accompanied by an increase in vertical deflections. Conversely, for a given deflection, the central tensile area is expected to increase with an increase in the reinforcement area. In the studies so far, slab panels (composite beam-slab systems) have been discussed. The slab behaviour is therefore the result of contributions from both the reinforcement and the composite beams. An attempt is now made to quantify the effects of reinforcement alone on slab capacity at elevated temperatures. Fig. 13(a) shows the variation of the central tensile area of three square concrete slabs (6m x 6m, 9m x 9m and 12m x 12m) with reinforcement area. The results are shown for a span/deflection ratio of 20. The slabs are 120mm thick, have an isotropic reinforcement mesh at an average depth of 60mm from the top surface of the slab, support a load of 3.11kN/m^2, and are supported on simple vertical supports. The slabs have the same reinforcement yield strength of 500MPa. The reinforcement mesh sizes are 142, 166, 221, 252, 284, 318, 354 and 393 mm^2/m in each orthogonal direction. The results are obtained by examining the membrane traction results in the *Vulcan* (Huang *et al.*, 2003a, 2003b, 2004a) analyses, and determining the transition points between tensile and compressive tractions. In Fig. 13 the radius of the tensile traction for each reinforcement area is indicated by triangles for 12m x 12m; squares for 9m x 9m and

diamonds for 6m x 6m slabs. Third-order polynomials are then fitted to the data to observe the trends. From Fig. 13(a), the 9m x 9m and 12m x 12m slabs show that the radius of the tensile region reduces with increasing reinforcement area, while the 6m x 6m slab indicates the opposite. Fig. 13(b) is a normalised form of the same results, which confirms this observation and further indicates that, beyond a 280mm^2/m mesh, the increase in reinforcement area has a negligible effect on the extent of the central area, and hence on the tensile capacity of the slab. Fig. 13(c) suggests an explanation of this behaviour. It shows the yield-line failure loads and the corresponding membrane enhancements at the times when the individual slabs attain a span/deflection ratio of 20. It can be seen that most of the 9m x 9m and 12m x 12m slabs had yield line failure loads below the applied loading (3.11kN/m^2), and therefore required significant enhancement to carry them. The results in Figs 13(a) and 13(b) therefore indicate that these slabs need to achieve large deflections to generate the membrane capacity required to bear the applied load. With each increase in reinforcement area the need for this enhancement reduces, and therefore the membrane capacity required to attain *span/20* deflection also reduces. With the 6m x 6m slab however, the context differs. The yield line failure loads are increasingly higher than those required to carry the applied load, until significant reductions in the reinforcement tensile strength force reductions in yield strengths beyond a reinforcement area of 250mm^2/m. The temperature of the 284mm^2/m reinforcement is 614°C at the point when the deflection of that slab reaches 300mm (*span/20*). The significant loss in yield strength thereafter requires a higher reinforcement area to generate the required 3.11kN/m^2 load capacity. Fig. 13 therefore suggests that for 'small' slabs an increase in reinforcement area has a positive influence on the slab's capacity (but heavy reinforcement makes little contribution), while large reinforcement areas are required, by default, for larger slabs.

4 Conclusions

The analyses and comparisons made in this investigation confirm a discrepancy between the original Bailey-BRE Method and its development to TSLAB, in their interpretation of deflection limits. The results also show that, even after recent development, the Bailey-BRE Method loses its conservatism with higher reinforcement ratios. The method's reliance on calculating the deflection required to enhance the traditional yield-line capacity, without adequate consideration of the stability of the

edge beams, results in very optimistic predictions of slab panel resistance with larger mesh sizes. On the other hand the finite element analyses show that, when load redistributions, aspect ratios and edge beam deflections are considered, only marginal increases in slab panel capacity are obtained with increasing reinforcement size, and the slab panel eventually fails by edge beam failure. The simple edge-beam collapse mechanism is found to give accurate predictions of slab panel runaway failure. The comparison indicates that this mechanism needs to be added to the Bailey-BRE Method, since edge beams do not stay cold throughout a fire.

Further analyses of the effect of reinforcement size on slab panel capacities reveals that, for small sized panels and lower fire resistance requirements, increasing reinforcement size does not significantly increase the panel capacity. However, it is simply logical that larger mesh sizes are required for large panels. Higher reinforcement ratios are also required for slabs designed for longer fire resistance periods, in order to resist the high initial thermal bending which occurs. In terms of membrane enhancement however, increasing the mesh size has little influence.

Acknowledgements

The authors would like to acknowledge the Overseas Research Studentship Award Scheme, the University of Sheffield and Corus PLC, which collectively funded this project.

References

Abu, A. K. *Behaviour of composite floor systems in fire*, PhD Thesis, University of Sheffield, Sheffield, 2009.

Abu, A. K., Burgess, I. W. and Plank, R. J. (2008). Slab panel vertical support and tensile membrane action in fire. *Steel and Composite Structures* **8**, No. 3, 217-230.

Bailey, C. G. *Design of Steel Structures with Composite Slabs at the Fire Limit State*, The Building Research Establishment, Garston, UK, 2000, Final Report No. 81415, for DETR and SCI.

Bailey, C. G. *Steel structures supporting composite floor slabs: design for fire*, The Building Research Establishment, Garston, UK, 2001, BRE Digest 462.

Bailey, C. G. (2003). Efficient arrangement of reinforcement for membrane behaviour of composite floors in fire conditions. *Journal of Constructional Steel Research* **59**, No. 7, 931-949.

Bailey, C. G. and Moore, D. B. (2000). The structural behaviour of steel frames with composite floor slabs subject to fire: Part 1: Theory. *The Structural Engineer* **78**, No. 11, 19-27.

Bailey, C. G. and Toh, W. S. (2007a). Behaviour of concrete floor slabs at ambient and elevated temperatures. *Fire Safety Journal* **42**, No. 6-7, 425-436.

Bailey, C. G. and Toh, W. S. (2007b). Small-scale concrete slab tests at ambient and elevated temperatures. *Engineering Structures* **29**, 2775-2791.

BSI British Standards. *Fire Tests on building materials and structures: Method for determination of the fire resistance of load bearing elements of construction*. BSI, London, 1987, BS 476: Part 21.

BSI British Standards. *Structural use of steelwork in building: Design in composite construction*. BSI, London, 1990, BS 5950: Part 3.

BSI British Standards. *Structural use of steelwork in building: Code of practice for fire resistant design*. BSI, London, 2003, BS 5950: Part 8.

BSI British Standards. *Design of composite steel and concrete structures: General rules – Structural fire design*. BSI, London, 2005, BS EN1994: Part 1-2.

Foster, S. J. *Tensile membrane action of reinforced concrete slabs at ambient and elevated temperatures*, PhD Thesis, University of Sheffield, Sheffield, 2006.

Foster, S. J., Bailey, C. G., Burgess, I. W. and Plank, R. J. (2004). Experimental behaviour of concrete floor slabs at large displacements. *Engineering Structures* **26**, 1231-1247.

Huang, Z., Burgess, I. W. and Plank, R. J. (2003a). Modelling Membrane Action of Concrete Slabs in Composite Buildings in Fire. I: Theoretical Development. *Journal of Structural Engineering ASCE* **129**, No. 8, 1093-1102.

Huang, Z., Burgess, I. W. and Plank, R. J. (2003b). Modelling Membrane Action of Concrete Slabs in Composite Buildings in Fire. II: Validations. *Journal of Structural Engineering ASCE* **129**, No. 8, 1103-1112.

Huang, Z., Burgess, I. W. and Plank, R. J. 3D Modelling of Beam-Columns with General Cross-Sections in Fire. *Proceedings of the 3rd International Workshop on Structures in Fire*, Ottawa, Canada, 2004a, **1**, 323-334.

Huang, Z., Burgess, I. W. and Plank, R. J. (2004b). Fire resistance of composite floors subjected to compartment fires. *Journal of Constructional Steel Research* **60,** No.2, 339-360.

Huang, Z., Burgess, I. W., Plank, R. J. and Bailey, C. G. Comparison of BRE Simple Design Method for Composite Floor Slabs in Fire with Non-Linear FE Modelling. *Proceedings of the 2nd International Workshop on Structures in Fire*, Christchurch, New Zealand, 2002, **1**, 83-94.

Huang, Z., Platten, A. and Roberts, J. (1996). Non-linear Finite Element Model to Predict Temperature Histories within Reinforced Concrete in Fires. *Building and Environment* **31**, No.2, 109-118.

Newman, G. M., Robinson, J. T. and Bailey, C. G. *Fire Safe Design: A New Approach to Multi-Storey Steel-Framed Buildings*, 2nd Edition, The Steel Construction Institute, UK, 2006, SCI Publication P288

Toh, W. S. and Bailey, C. G. Comparison of simple and advanced models for predicting membrane action on long span slab panels in fire. Proceedings of the 11th International Fire Science and Engineering Conference (Interflam 2007), London, UK, 2007, 791-796

Figure Captions

Fig. 1: Schematic diagram of the Bailey-BRE Method.

Fig. 2: Slab deflection limits.

Fig. 3: Slab panel sizes.

Fig. 4: Concrete slab cross-section, showing the trapezoidal decking profile.

Fig. 5: Slab panel folding mechanism.

Fig. 6: Beam and slab temperature evolution for R60 design.

Fig. 7a: Bailey-BRE Method - 9m x 6m slab panel. Required vertical displacements (R60).

Fig. 7(b): *Vulcan* – 9m x 6m slab panel. Central vertical displacements (R60).

Fig. 7(c): *Vulcan* – 9m x 6m slab panel. Displacements of slab centre relative to protected secondary beams (R60).

Fig. 8(a): Bailey-BRE Method - 9m x 12m slab panel. Required vertical displacements (R60).

Fig. 8(b): *Vulcan* – 9m x 12m slab panel. Central vertical displacements (R60).

Fig. 8(c): *Vulcan* – 9m x 12m slab panel. Displacements of slab centre relative to protected secondary beams (R60).

Fig. 9(a): Bailey-BRE Method - 9m x 9m slab panel. Required vertical displacements (R60).

Fig. 9(b): *Vulcan* – 9m x 9m slab panel. Central vertical displacements (R60).

Fig. 9(c): *Vulcan* – 9m x 9m slab panel. Displacements of slab centre relative to protected secondary beams (R60).

Fig. 10(a): Bailey-BRE and *Vulcan* 9m x 6m slab panel comparison (R60).

Fig. 10(b): Bailey-BRE and *Vulcan* 9m x 12m slab panel comparison (R60).

Fig. 10(c): Bailey-BRE and *Vulcan* 9m x 9m slab panel comparison (R60).

Fig. 11(a): *Vulcan* normalised failure times vs. reinforcement area – 9m x 6m slab panel.

Fig. 11(b): *Vulcan* normalised failure times vs. reinforcement area – 9m x 12m slab panel.

Fig. 11(c): *Vulcan* normalised failure times vs. reinforcement area – 9m x 9m slab panel.

Fig. 12: *Vulcan* – 9m x 12m slab panel central vertical displacements (R120).

Fig. 13(a): *Vulcan* – Variation of radius of central tensile area with reinforcement area.

Fig. 13(b): *Vulcan* – Normalised variation of radius of central tensile area with reinforcement area.

Fig. 13(c): Yield-line loads and enhancement factors for the slab results in Figs. 13(a) and 13(b).

Table Captions

Table 1: Slab panel requirements (R60).

Table 2: Protected beam design data (R60).

Table 3: Slab panel failure times and corresponding secondary beam temperatures (R60).

Table 4: Protected beam design data for R90 and R120.

Table 5: Slab panel failure times and corresponding secondary beam temperatures (R90 and R120).

Tables

Table 1: Slab panel requirements (R60)

Slab Panel size	9m x 6m	9m x 9m	9m x 12m
Dead load (kN/m^2)	4.33	4.33	4.33
Live load (kN/m^2)	5.0	5.0	5.0
Additional load (kN)	14	37	49
Beam design factor	0.77	1.00	0.83
Min. Mesh size	A193	A193	A252

Table 2: Protected beam design data (R60)

Slab Panel Size	Beam Type	Beam Section	Load Ratio	Limiting Temperature	Temperature at 60 minutes
9m x 6m	Secondary	356 x 171 x 57 UB	0.426	636°C	548°C
	Primary	406 x 178 x 60 UB	0.452	627°C	549°C
9m x 9m	Secondary	356 x 171 x 67 UB	0.442	630°C	550°C
	Primary	533 x 210 x 101 UB	0.446	629°C	548°C
9m x 12m	Secondary	406 x 178 x 67 UB	0.447	629°C	548°C
	Primary	610 x 305 x 179 UB	0.471	620°C	547°C

Table 3: Slab panel failure times and corresponding secondary beam temperatures (R60)

	Slab panel	Failure Time	Intermediate beam temperature	Secondary beam temperature
R60	9m x 6m	82min	983°C	663°C
	9m x 9m	73min	963°C	621°C
	9m x 12m	68min	952°C	594°C

Table 4: Protected beam design data for R90 and R120

	Slab Panel Size	Beam Type	Beam Section	Load Ratio	Limiting Temperature	R90 or R120 temperature
R90	9m x 6m	Secondary	356 x 171 x 57 UB	0.440	631°C	549°C
		Primary	406 x 178 x 60 UB	0.453	627°C	549°C
	9m x 9m	Secondary	356 x 171 x 67 UB	0.451	627°C	550°C
		Primary	533 x 210 x 101 UB	0.447	628°C	549°C
	9m x 12m	Secondary	406 x 178 x 67 UB	0.470	621°C	549°C
		Primary	610 x 305 x 179 UB	0.473	620°C	549°C
R120	9m x 6m	Secondary	356 x 171 x 57 UB	0.445	629°C	549°C
		Primary	406 x 178 x 60 UB	0.453	626°C	550°C
	9m x 9m	Secondary	356 x 171 x 67 UB	0.459	624°C	550°C
		Primary	533 x 210 x 101 UB	0.452	627°C	549°C
	9m x 12m	Secondary	457 x 152 x 67 UB	0.447	629°C	550°C
		Primary	686 x 254 x 170 UB	0.454	626°C	550°C

Table 5: Slab panel failure times and corresponding secondary beam temperatures (R90 and R120)

	Slab panel	Failure Time	Intermediate beam temperature	Secondary beam temperature
R90	9m x 6m	124min	1051°C	673°C
	9m x 9m	113min	1036°C	637°C
	9m x 12m	101min	1018°C	593°C
R120	9m x 6m	163min	1103°C	673°C
	9m x 9m	148min	1083°C	634°C
	9m x 12m	136min	1067°C	601°C

Figures

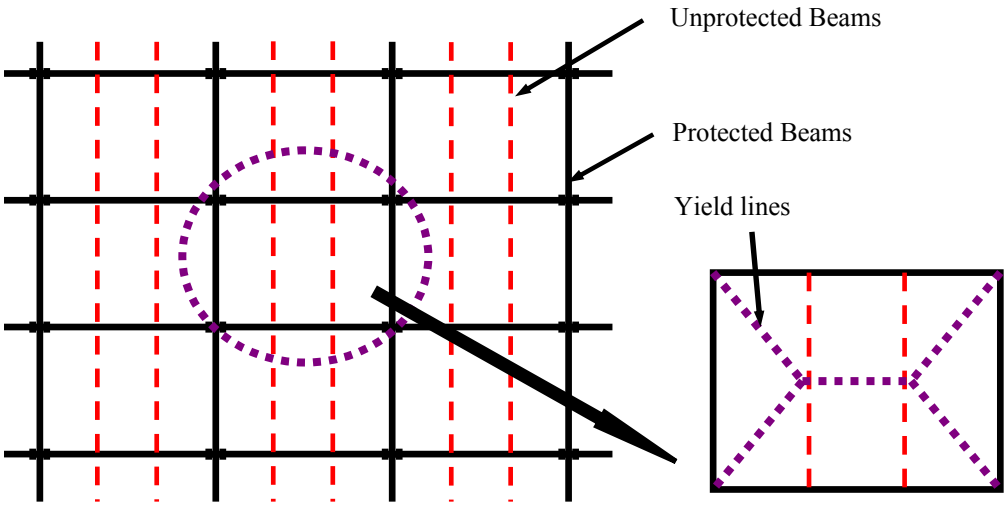

Fig. 1: Schematic diagram of the Bailey-BRE Method

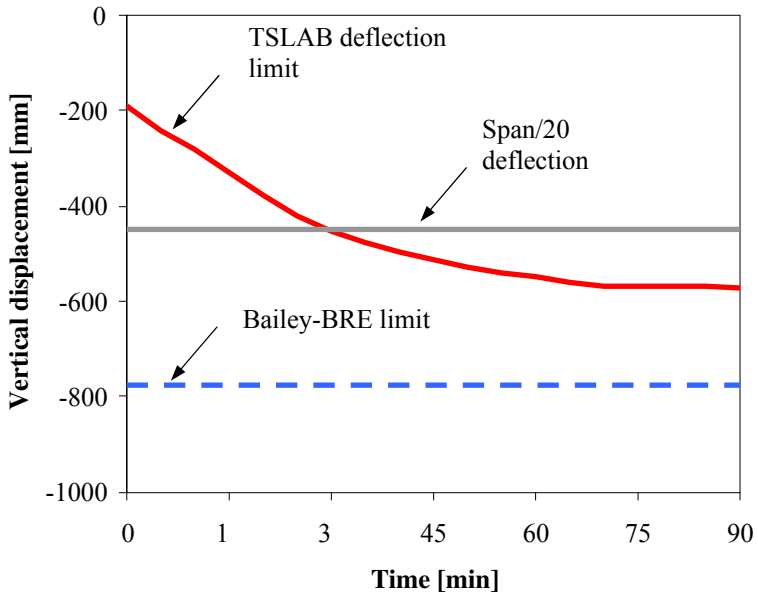

Fig. 2: Slab deflection limits

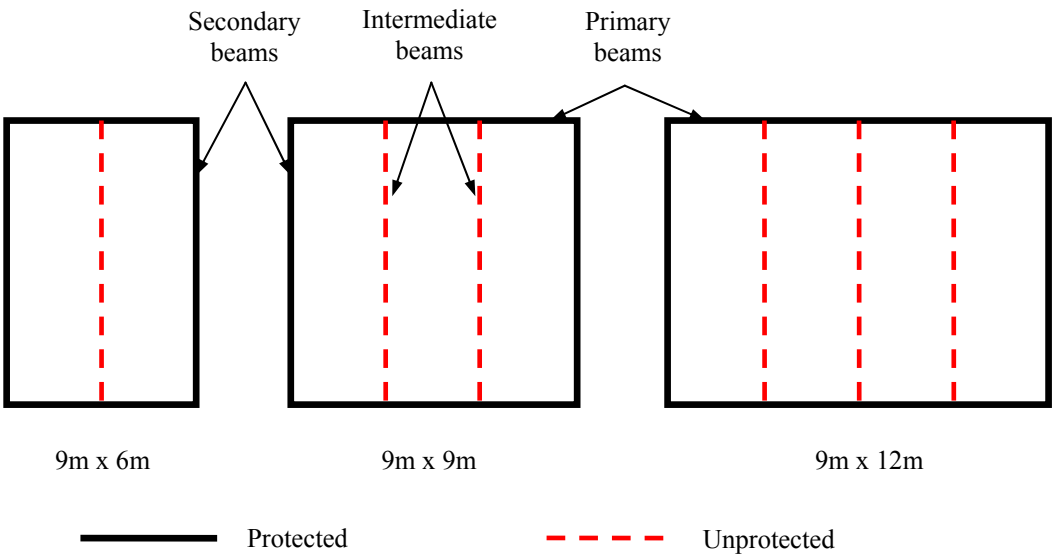

Fig. 3: Slab panel sizes

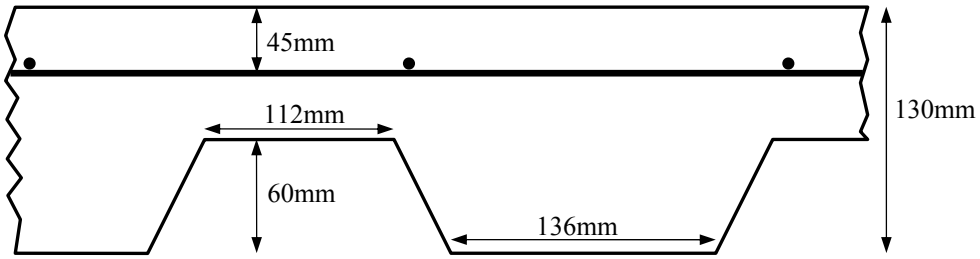

Fig. 4: Concrete slab cross-section, showing the trapezoidal decking profile

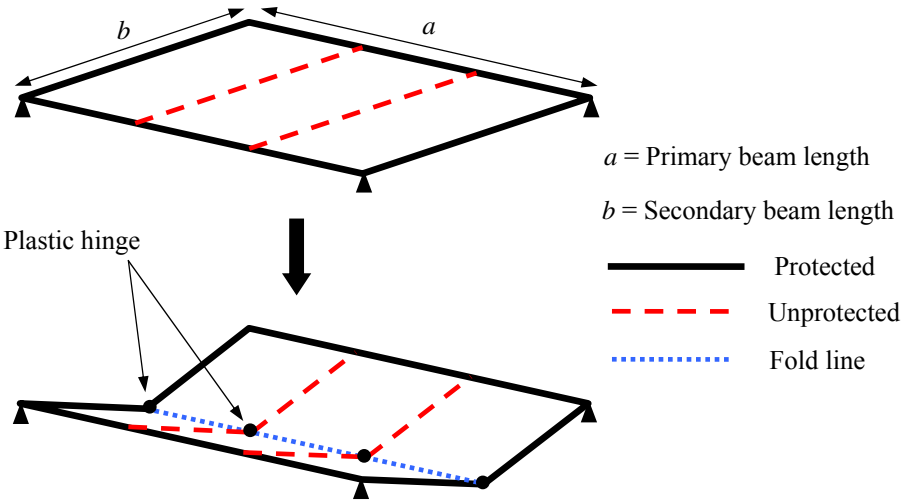

Fig. 5: Slab panel folding mechanism

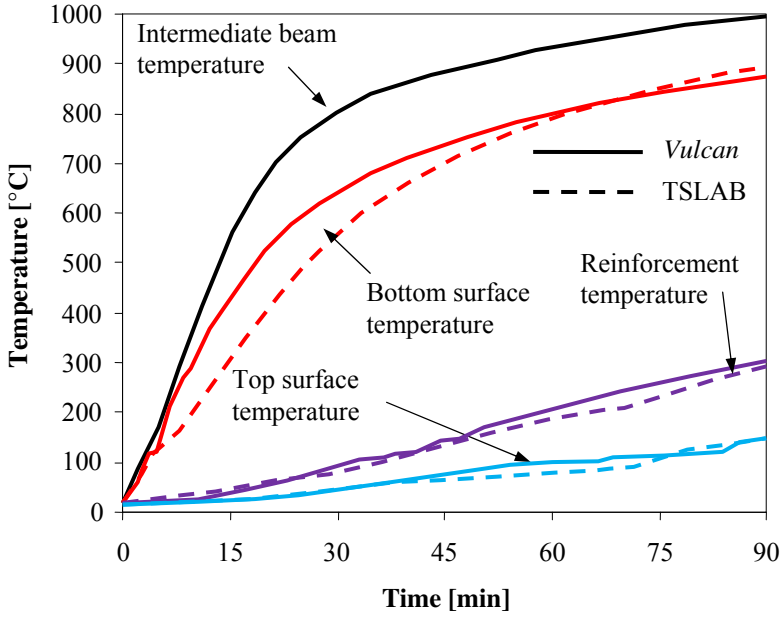

Fig. 6: Beam and slab temperature evolution for R60 design

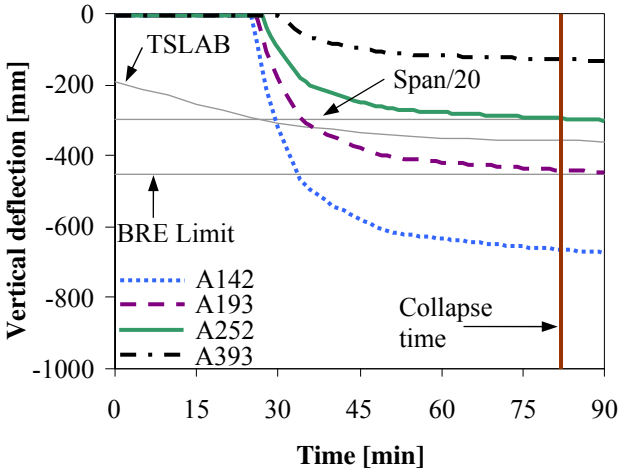

Fig. 7(a): Bailey-BRE Method - 9m x 6m slab panel. Required vertical displacements (R60)

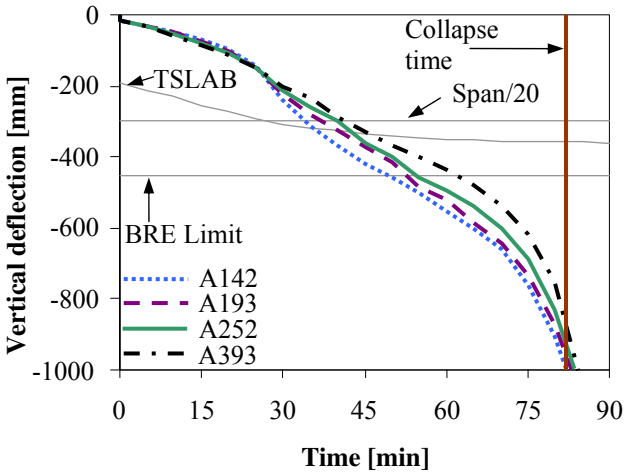

Fig. 7(b): *Vulcan* – 9m x 6m slab panel. Central vertical displacements (R60)

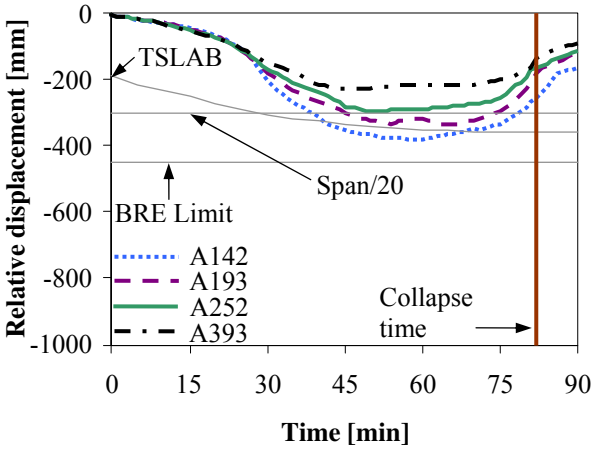

Fig. 7(c): *Vulcan* – 9m x 6m slab panel. Displacements of slab centre relative to protected secondary beams (R60).

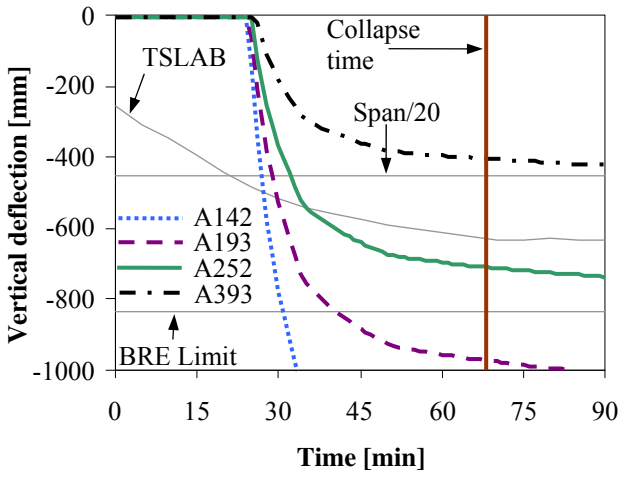

Fig. 8(a): Bailey-BRE Method - 9m x 12m slab panel. Required vertical displacements (R60)

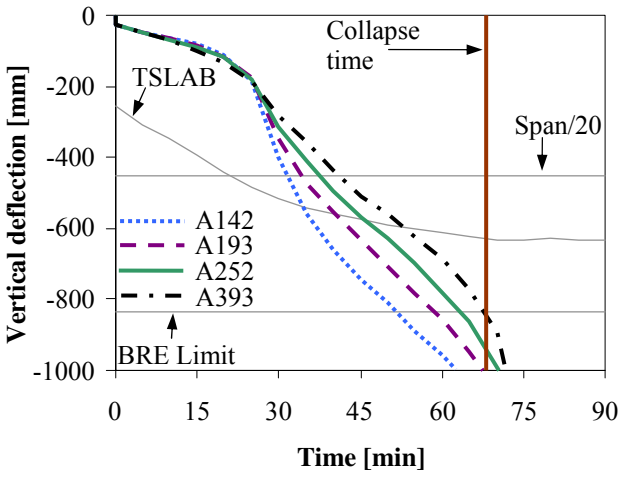

Fig. 8(b): *Vulcan* – 9m x 12m slab panel. Central vertical displacements (R60)

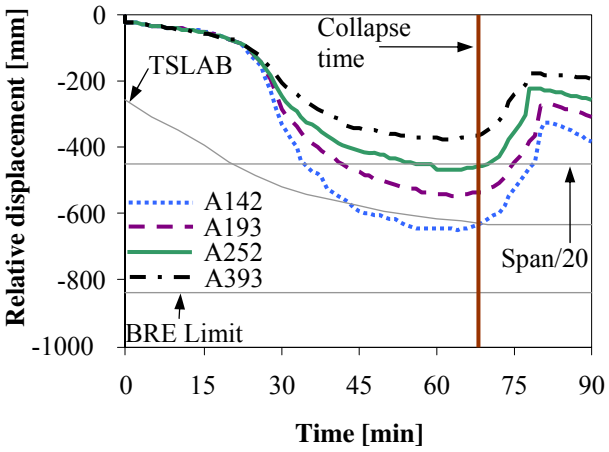

Fig. 8(c): *Vulcan* – 9m x 12m slab panel. Displacements of slab centre relative to protected secondary beams (R60)

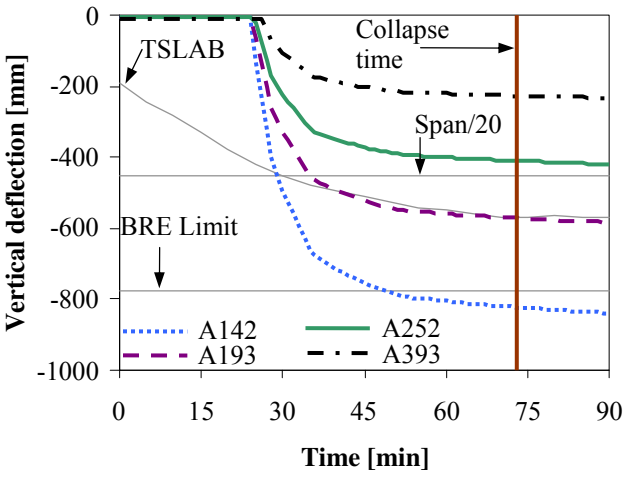

Fig. 9(a): Bailey-BRE Method - 9m x 9m slab panel. Required vertical displacements (R60)

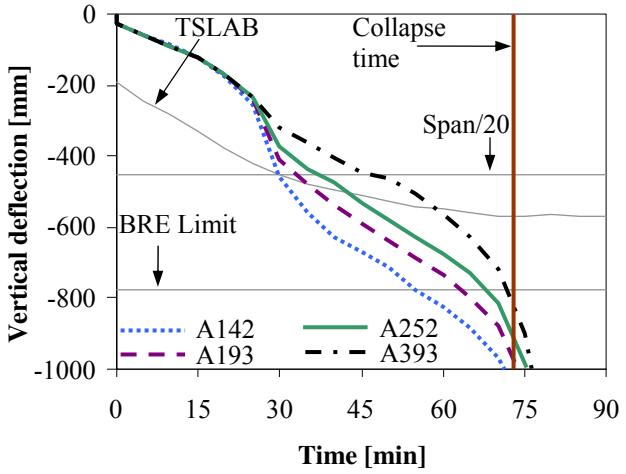

Fig. 9(b): *Vulcan* – 9m x 9m slab panel. Central vertical displacements (R60)

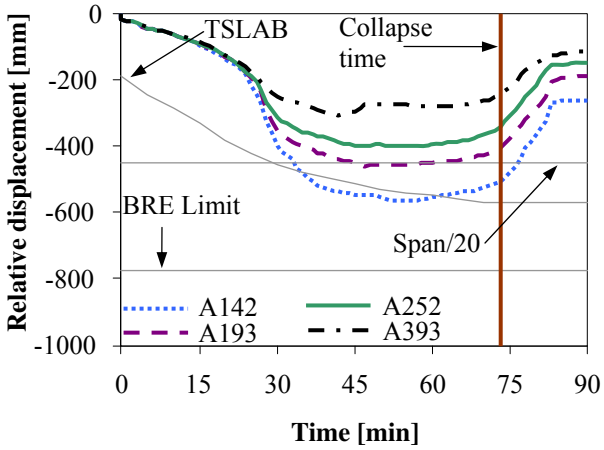

Fig. 9(c): *Vulcan* – 9m x 9m slab panel. Displacements of slab centre relative to protected secondary beams (R60)

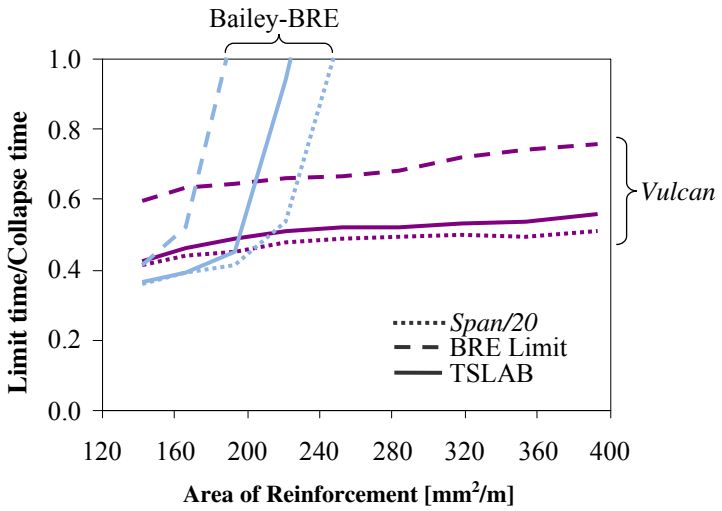

Fig. 10(a): Bailey-BRE and *Vulcan* 9m x 6m slab panel comparison (R60)

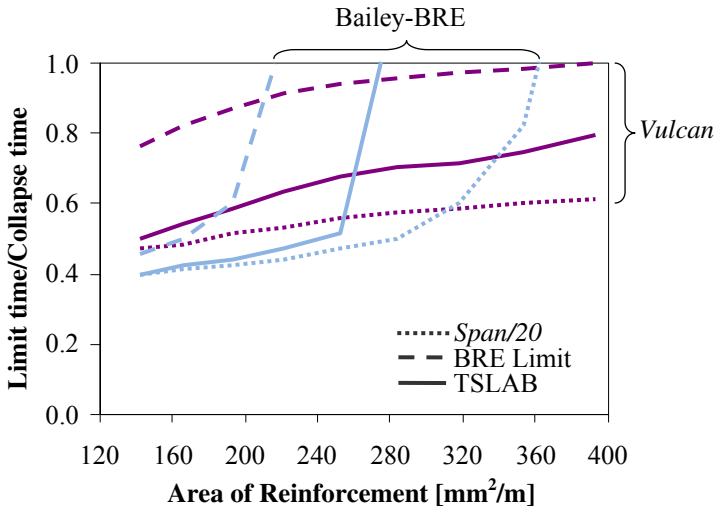

Fig. 10(b): Bailey-BRE and *Vulcan* 9m x 12m slab panel comparison (R60)

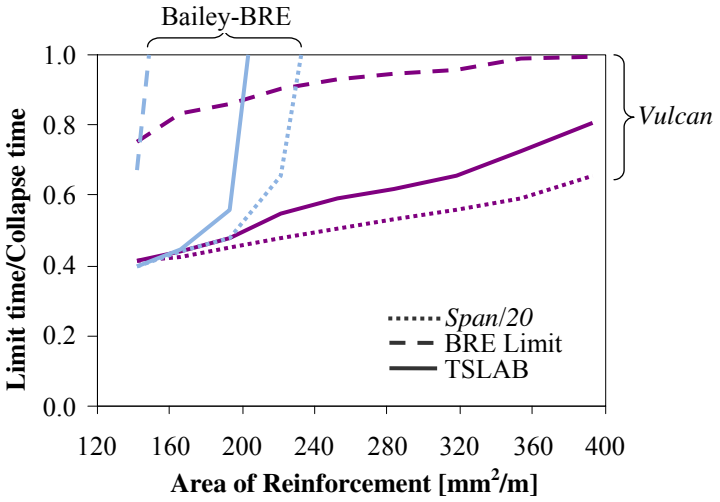

Fig. 10(c): Bailey-BRE and *Vulcan* 9m x 9m slab panel comparison (R60)

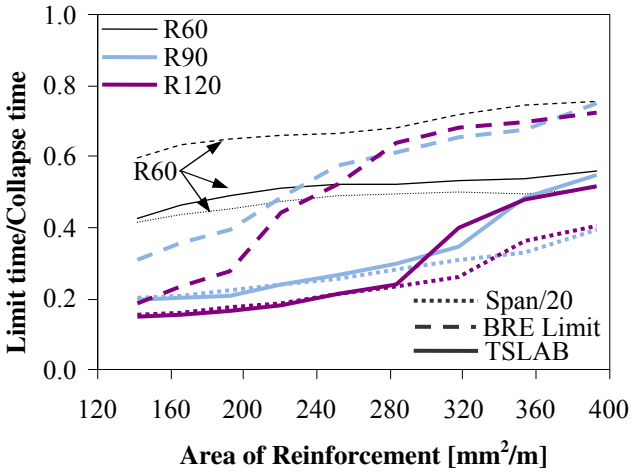

Fig. 11(a): *Vulcan* normalised failure times vs. reinforcement area – 9m x 6m slab panel.

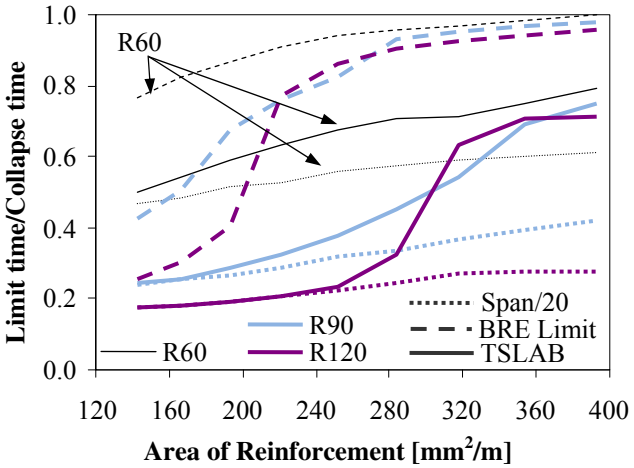

Fig. 11(b): *Vulcan* normalised failure times vs. reinforcement area – 9m x 12m slab panel.

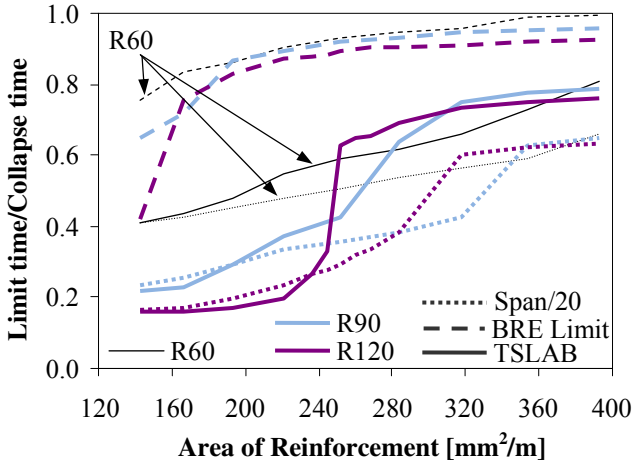

Fig. 11(c): *Vulcan* normalised failure times vs. reinforcement area – 9m x 9m slab panel

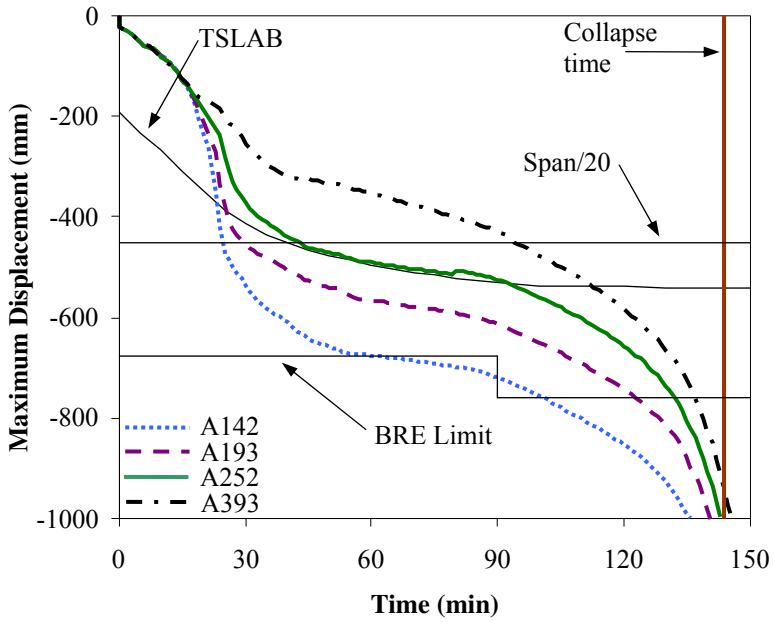

Fig. 12: *Vulcan* – 9m x 12m slab panel central vertical displacements (R120)

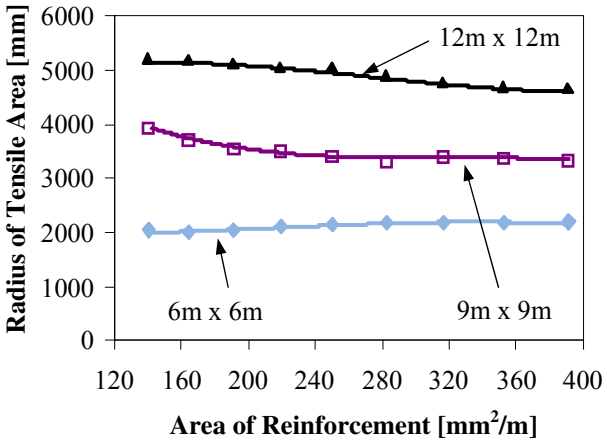

Fig. 13(a): *Vulcan* – Variation of radius of central tensile area with reinforcement area

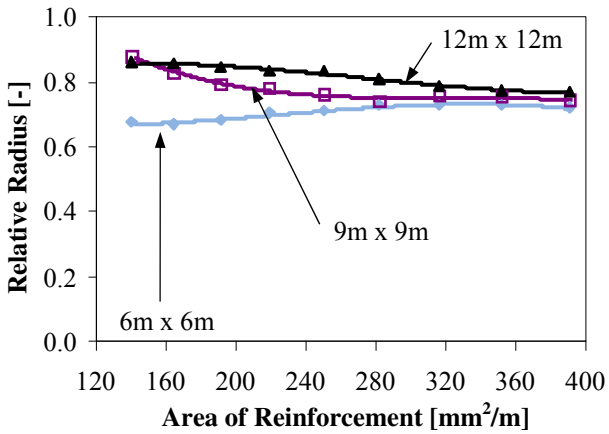

Fig. 13(b): *Vulcan* – Normalised variation of radius of central tensile area with reinforcement area

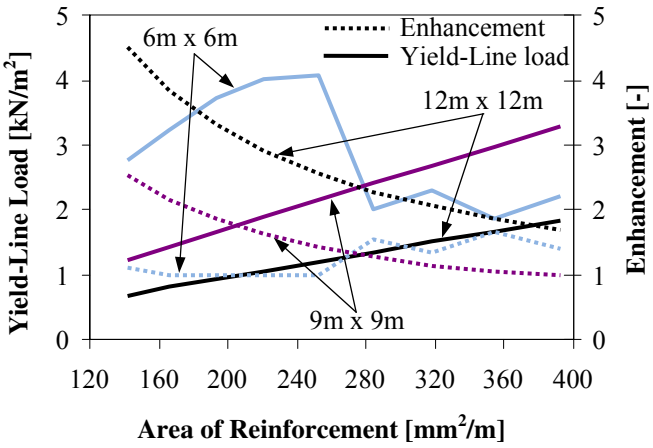

Fig. 13(c): Yield-line loads and enhancement factors for the slab results in Figs. 13(a) and 13(b)